The International Journal of Advanced Manufacturing Technology (2018) 97:711–722
https://doi.org/10.1007/s00170-018-1877-1

ORIGINAL ARTICLE

Effect of cutting edge radius on micro end milling: force analysis, surface roughness, and chip formation

K. Vipindas[1] · K. N. Anand[1] · Jose Mathew[1]

Received: 5 October 2016 / Accepted: 12 March 2018 / Published online: 12 April 2018

Abstract
Producing miniaturized components from a wide variety of engineering materials is one of the most important fields of interest in manufacturing industry. Micro end milling is considered to be one of the efficient methods to produce complex 3D micro components. In micro machining, undeformed chip thickness is comparable to the tool edge radius, which introduces a critical undeformed chip thickness. Below the regime of critical undeformed chip thickness material is not removed but plowed. Ti-6Al-4V is one of the most popular titanium alloy because of its superior properties such as resistance to heavy loads, corrosion resistance, lightness, and bio-compatibility. This paper investigates micro end milling characteristics of the Ti-6Al-4V titanium alloy through a series of cutting experiments. Here the size effect in micro end milling was observed by studying the effect of the cutting edge radius on process performance. In order to understand the effect of the cutting edge radius on machining performance, range of feed per tooth was selected in such a way that it includes both within and outside the size effect region. This paper explores how cutting edge radius affects the cutting force, coefficient of friction, surface roughness, and chip formation during the micro end milling process. A size effect region was obtained from the variation of cutting force with feed per tooth. It was found that feed per tooth in the vicinity of 1-μm range is critical feed per tooth value, which is approximately one third of the cutting edge radius. Below this value, the cutting edge radius effect is predominant which would result in more ploughing mechanism. This was evident from the deviation of cutting force from the linear trend, increase in coefficient of friction, and surface roughness value at lower feed per tooth. In addition, a cutting force model was proposed considering the cutting edge radius effect and has been validated with experimental results.

Keywords Micro end milling · Cutting force · Coefficient of friction · Surface roughness · Chip geometry

1 Introduction

The need for smaller and reliable engineering components has given rise to more stringent requirements on micro fabrication processes. Micro end milling process is one of the preferred methods to manufacture the miniature components. Advantages of the micro end milling process over other micro manufacturing processes are low cost, high material removal rate, material compatibility, and flexibility to produce complex micro 3D parts such as micro dies and molds. Initially, micro end milling was used in electronics and aerospace industry and later on it was introduced into biomedical industry. The micro milling process utilizes end mills with diameter in the range of 25 to 1000 μm having up to 20 μm cutting edge radius [1]. Additionally, the micro milling process has several salient features that differentiate it from the macro milling process. In the micro end milling process, the feed per tooth will be comparable to the cutting edge radius, which brings size effect to the machining process. Therefore, many factors which are insignificant in the conventional milling process will become significant in the micro milling process.

Cutting force prediction at micro-scale machining is an important research field in order to enable the correct choice of cutting parameters, correct design of micro tools, and estimation of machining tolerances. It is very important to study the cutting forces during micro end milling process for proper

✉ K. Vipindas
vipindas.k@gmail.com

K. N. Anand
anandkrish487@gmail.com

Jose Mathew
josmat@nitc.ac.in

[1] Mechanical Engineering Department, NIT Calicut, Kozhikode, India

planning and control of machining process and for optimizing the cutting condition. Cutting force analysis plays an important role in studying various characteristics of any machining process, such as quality of the machined surface, positioning accuracy, and tool life, as stated by Zaman et al. [2]. As mentioned in [3, 4], when machining within the size effect zone, ploughing effect is predominant which results in increase in cutting force and thereby increases surface roughness value. Therefore, force modeling of micro end milling process is very important to understand the process and to improve the tool life as well as the part quality.

Like in any micro machining process, the cutting edge radius of the micro end mill will be comparable with the size of uncut chip thickness [5]. No chip is formed when the uncut chip thickness is below the minimum uncut chip thickness (MUCT) [6]. Under this condition, a part of workpiece material will plastically deform and the remaining part elastically recovers. This change in chip formation is known as the minimum chip thickness effect. This will result in an increase in cutting force [3, 7] and surface roughness value as proposed by Vogler et al. [8]. Since MUCT plays an important role in the micro machining mechanism, a number of studies have been concentrated on finding MUCT both experimentally and numerically. Liu et al. [9] and Malekian et al. [10] developed a model to predict the MUCT during the micro machining process. Zhanqiang et al. [11] determined MUCT numerically as well as experimentally. It was found that MUCT increases with cutting edge radius and the minimum surface roughness value was achieved when machining at MUCT. de Oliveira et al. [12] suggested that the minimum chip thickness for micro milling varied from one fourth to one third of the cutting edge radius, irrespective of workpiece material, tool, and machining parameter.

Some researchers [4, 13] have investigated the size effect during the micro milling process by studying the effect of the ratio of undeformed chip thickness to the cutting edge radius on process performance such as specific cutting forces, surface roughness, and burr formation. It was found that the minimum surface roughness value was observed when the undeformed chip thickness is the same as the tool edge radius. Figure 1 shows the basic mechanism of the micro machining process under different conditions of undeformed chip thickness [4].

Lee and Lin [14] studied the plastic deformation and fracture behavior of Ti-6Al-4V under constant strain rates at temperature ranging from room temperature to 1000 °C. Mamedov and Lazoglu [15] have developed a model for predictions of the thermal fields in micro milling. The estimated temperatures were validated by the temperature measurements with thermocouples at specific points. The temperature distribution in the tool and the workpiece was estimated using the heat generated in the primary and secondary deformation zones.

Study and modeling of forces in micro end milling have been in the focus in recent time. Some of the researchers have concentrated on empirical [16] and FEM-based approach [17] for force modeling. There are few mechanistic force models [18–22] developed for the micro end milling process. Jun et al. [18] have proposed a mechanistic force model considering both shearing-dominant and ploughing-dominant regimes. Jin and Altintas [1] predicted micro milling forces with the orthogonal model. They have used a 2D finite element model for the prediction of micro end milling forces while machining brass. Series of finite element simulations were used to evaluate the cutting force coefficients which were then used to obtain the cutting forces. Afazov et al. [23] predicted micro milling cutting forces through 2D finite element simulation of orthogonal cutting. The effect of uncut chip thickness, cutting velocity, and edge radius was included.

Despite the large number of research being done in the micro end milling process, there is still a significant gap in understanding the micro milling process at different cutting conditions. Basic understanding of cutting force, chip formation, surface finish, and coefficient of friction during micro machining and deviation of these responses from the conventional macro scale machining process are lacking. Apart from this, there is a need to investigate micro machining of difficult to cut materials such as titanium alloys as it finds applications in various engineering fields. Since titanium alloys account for approximately 30% of the material in aero engines, it is considered to be the most influential material in aerospace industry. Nowadays, titanium alloys are finding applications in other fields such as optics, electronics, and communications.

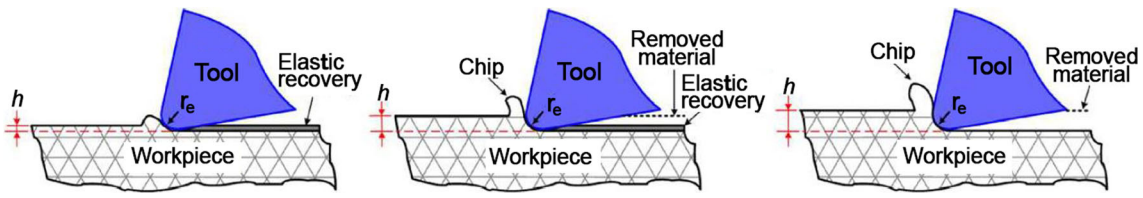

(a) h < MUCT (b) h ≈ MUCT (c) h > MUCT

Fig. 1 Basic mechanism of chip formation in micro-scale machining. **a** h < MUCT. **b** h ≈ MUCT. **c** h > MUCT [4]. © Elsevier. Reproduced by permission of Elsevier. Permission to reuse must be obtained from the rights holder

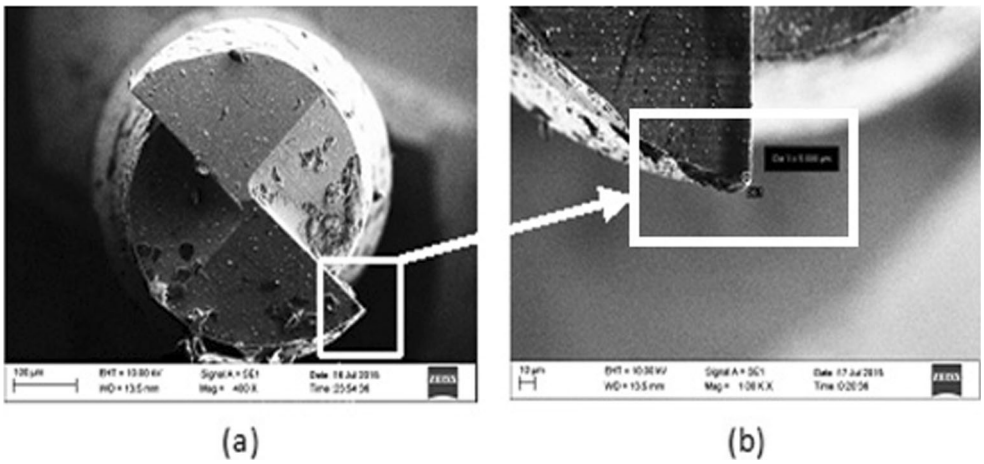

Fig. 2 SEM images of a new (a) micro end mill cutter and (b) cutter edge radius

However, titanium alloys are known to be one of the difficult to machine material due to following reasons: (a) low thermal conductivity, (b) high chemical reactivity with many tool materials, and (c) rapid tool wear.

The objective of this paper is to explore the effect of the cutting edge radius on various machining performance such as cutting force, coefficient of friction, surface roughness, and chip formation during the micro end milling process. Experiments were conducted for wide range of feed per tooth (0.2, 0.4, 0.6, 1, 2, 3, 4 μm) on Ti-6Al-4V with fresh tools for each experimental condition so that the effect of tool wear can be minimized. While selecting range of feed per tooth, care has been taken such that it includes both within and outside the size effect region to understand the influence of cutting edge radius on the micro end milling process. Apart from this, a cutting force model considering the cutting edge radius effect during the micro end milling process has been presented and validated with the experimental results.

2 Experimental setup

2.1 Workpiece material

Ti-6Al-4V is one of the most popular titanium alloys, which is widely being used in many fields such as fabrication of aircraft structures, turbine blades, and medical implants, because of its superior properties such as resistance to heavy loads, great resistance to corrosion, lightness, high specific ultimate tensile strength, bio-compatibility, low thermal and electrical conductivity, and good thermal stability because of its moderately high melting point. Since titanium-base alloys are difficult to machine materials, its use is limited due to high production cost involved. In this study, Ti- 6Al-4V has been selected as the workpiece material.

2.2 Cutting tool

In this study, a tungsten carbide micro end mill tool with 1000 μm diameter and 0° rake angle (MAKE: UNION TOOLS – UT DRY C-CHES 2010-0400) was used as shown in Fig. 2. In micro machining, the cutting edge radius plays an important role on various machining parameters such as cutting force, surface finish, chip formation, and power consumption. Therefore, even though micro end mill with sharp edge has been selected for this study, it is necessary to measure the actual cutting edge radius of the tool. A scanning electron microscope (SEM) was used for measuring the cutting edge radius of the tool. Figure 2 shows the (a) micro end mill cutter and (b) SEM image of cutter edge. The cutting edge radius was measured in the range of 3–4 μm. This was done by fitting a circle to the SEM image of the cutter edge and the radius of the circle was taken as the cutting edge radius of the tool as shown in Fig. 2. Figure 3 shows the tool specification used in the experiments.

2.3 Experimental setup

Experiments were conducted using a micro machining center (DT110, Mikrotools, Singapore). Micro slots of 20 mm length

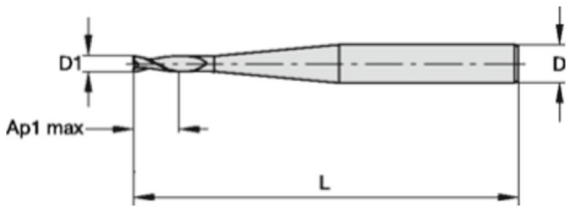

Fig. 3 Tool specifications

Dimensions in mm				No. of flutes	Helix angle
D1	D	Ap1 max	L		
1.0	4	4	45	2	30^0

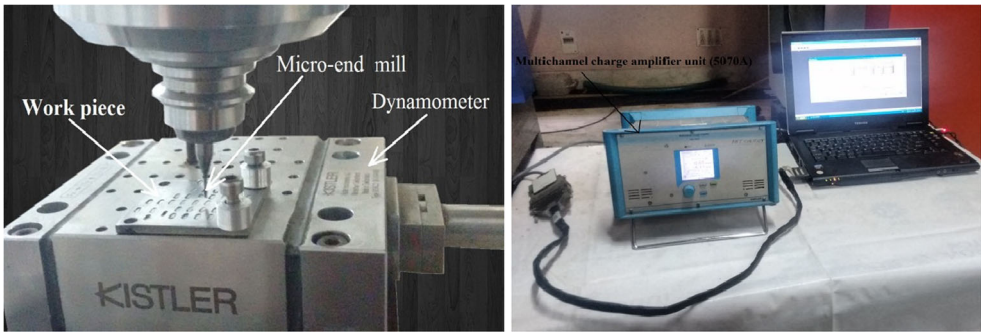

Fig. 4 Experimental setup

were machined on the Ti-6Al-4V workpiece to study the effect of feed per tooth on cutting force, coefficient of friction, surface roughness, and chip geometry.

Mini Dyn multicomponent Dynamometer (KISTLER Type 9256C2) interfaced to multichannel charge amplifier 5070A was used to measure cutting force during the micro end milling process. Workpiece was mounted directly on to the dynamometer. The configuration of experimental setup for measuring the cutting force during the micro end milling process is shown in Fig. 4. Surface roughness was measured by using Surftest SJ – 410 (Mitutoyo) with 5 μm stylus tip diameter.

Table 1 shows the experimental conditions to analyze the effect of feed per tooth on cutting force, coefficient of friction, surface roughness, and chip geometry during micro end milling of Ti-6Al-4V. Since the machining center used has maximum spindle speed limited to 5000 rpm, the cutting speed has been restricted to 15.7 m/min. Also, as the main objective of this paper is to understand the effect of feed per tooth on the machining process, more emphasis has been given in selecting feed per tooth both within and outside the size effect region.

3 Cutting force model for micro end milling

Figure 5 shows the basic difference between macro cutting and micro cutting. From this figure, it is evident that the cutting edge radius has a significant effect on the cutting mechanism during micro machining. In the micro machining process, cutting is achieved through ploughing and shearing of material when the undeformed chip thickness is below and above minimum uncut chip thickness.

Two assumptions were made in this study to simplify micro-scale milling as follows:

(a) The first assumption is made to simplify the complicated 3D milling process (Fig. 6a) to a 2D process as shown in Fig. 6b. Since in micro milling, the depth of cut (DOC) used is small, effect of helix angle can be ignored.
(b) The second assumption is made to build a relationship between the simplified 2D milling process and orthogonal machining process. As in Fig. 6b, the deformation area is much smaller compared to the tool and workpiece since the diameter of the tool is much bigger than the machining zone. Therefore, the deformed area can be considered as the orthogonal machining process as shown in Fig. 6c, d.

In micro machining, there is a possibility of elastic recovery of the workpiece material, so tool work piece contact length can be obtained as in Eq. (1) [19].

$$L_f = \frac{S}{\sin\theta_f} \tag{1}$$

where S is the spring back which is equal to $k_1 r_e H/E$, k_1 is a constant, r_e is the tool cutting edge radius, H is the Vickers hardness, E is the material elastic modulus, and θ_f is the relief angle of tool.

Table 1 Experimental conditions

Machine tool	Micro machining center (DT 110, Singapore)
Cutting speed (m/min)	15.7
Depth of cut (mm)	0.1
Feed per tooth (μm)	0.2, 0.4, 0.6, 1, 2, 3, 4
Cutting tool	WC micro end mill cutter with 1000 μm cutter diameter (0° rake angle)
Workpiece material	Ti-6Al-4V
Dynamometer	KISTLER (9256C2)

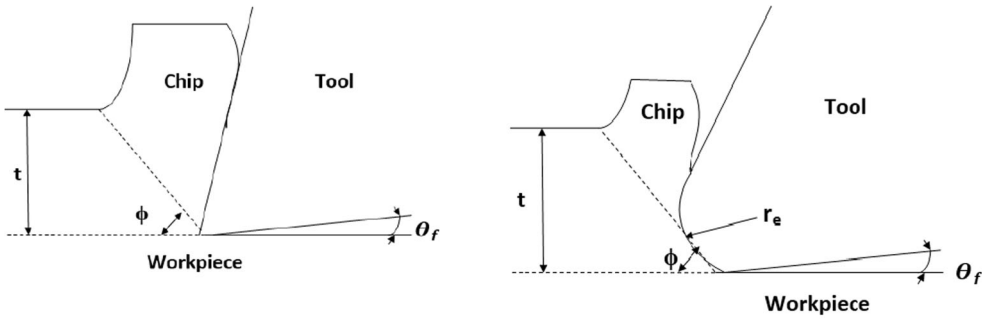

Fig. 5 Difference between **a** conventional macro and **b** micro cutting

When only the shear plane shear occurs, shear plane force (F_s) and shear plane normal force (N_s) can be expressed as

$$F_s = \frac{(\sigma/\sqrt{3})\, b\, t}{\sin\phi} \tag{2}$$

$$N_s = \frac{\sigma\, b\, t}{\sin\phi} \tag{3}$$

where b is the width of cut, t is the uncut chip thickness in orthogonal cutting, ϕ is the shear angle, and σ is the flow stress of the workpiece material.

In order to consider the spring back effect of workpiece material during micro machining, an additional frictional force owing to increase in work piece–tool contact length has been included in the force model as flank face contact force (F_{fc}) and flank face normal force (F_{ft}). This can be obtained as given in Eq. (4) and Eq. (5) [19].

$$F_{fc} = \frac{C\ Y}{\sqrt{3}} L_f\ \ b \tag{4}$$

$$F_{ft} = C\ \ Y\ \ L_f\ \ b \tag{5}$$

Combining above friction force components, the principal cutting force and thrust cutting force obtained from Merchant's circle diagram can be modified as in Eq. (6) and Eq. (7).

$$F_c = F_s\cos\phi + N_s\sin\phi + F_{fc} \tag{6}$$

$$F_t = -F_s\sin\phi + N_s\cos\phi + F_{ft} \tag{7}$$

For the micro end milling/end milling process, chip thickness varies with tool rotation angle, so chip thickness (t) can be written as a function of tool rotation angle as given in Eq. (8).

$$t = f_t\sin\theta \tag{8}$$

where f_t is the feed per tooth and θ is the tool rotation angle. By incorporating t in Eq. (2) and Eq. (3) and using Eq. (4) and Eq. (5), the final expression for principal cutting force and thrust force can be obtained. An expression for F_x and F_y was derived [19] as given below:

$$F_x = [C_1(\sin^2\theta_e - \sin^2\theta_s) + C_2(\sin 2\theta_e - \sin 2\theta_s) - C_4(\sin\theta_e - \sin\theta_s) + C_5(\cos\theta_e - \cos\theta_s) + C_3(\theta_e - \theta_s] \tag{9}$$

$$F_y = [C_3(\sin^2\theta_e - \sin^2\theta_s) + 0.5C_1(\sin 2\theta_e - \sin 2\theta_s) - C_5(\sin\theta_e - \sin\theta_s) - C_4(\cos\theta_e - \cos\theta_s) - C_1(\theta_e - \theta_s] \tag{10}$$

where

$$C_1 = -\frac{\sigma f_t r\cos\phi}{2\sqrt{3}\sin\phi\tan\psi} - \frac{\sigma f_t r}{2\tan\psi}$$

$$C_2 = -\frac{\sigma f_t r}{4\sqrt{3}\tan\psi} + \frac{\sigma f_t r\cos\phi}{4\sin\phi\tan\psi}$$

$$C_3 = \frac{\sigma f_t r}{2\sqrt{3}\tan\psi} - \frac{\sigma f_t r\cos\phi}{2\sin\phi\tan\psi}$$

$$C_4 = \frac{YL_f r}{\sqrt{3}\tan\psi},\quad C_5 = \sqrt{3}C_4$$

θ_s and θ_e are the tool start angle and tool end angle, respectively.ψ is the helix angle of the tool, r is the tool radius and shear angle (ϕ) can be obtained from Merchant's equation as given in Eq. (11). Based on the assumptions stated before, the effect of the helix angle can be ignored in the micro end milling process. Also, from the second assumption, it is reasonable to assume the micro end milling process as an orthogonal process. Therefore, by using Eq. 12, the coefficient of friction, μ, can be found out and then friction angle, λ, can be obtained from μ.

$$\phi = \frac{\pi}{4} + \frac{\alpha}{2} - \frac{\lambda}{2} \tag{11}$$

$$\mu = \frac{F_t + F_c\tan\alpha}{F_c - F_t\tan\alpha} \tag{12}$$

$$\lambda = \tan^{-1}\mu \tag{13}$$

where α is the tool rake angle. In this study, the nominal rake angle of the tool used is 0^0. But during the micro end milling process, the cutting edge radius plays an important role in

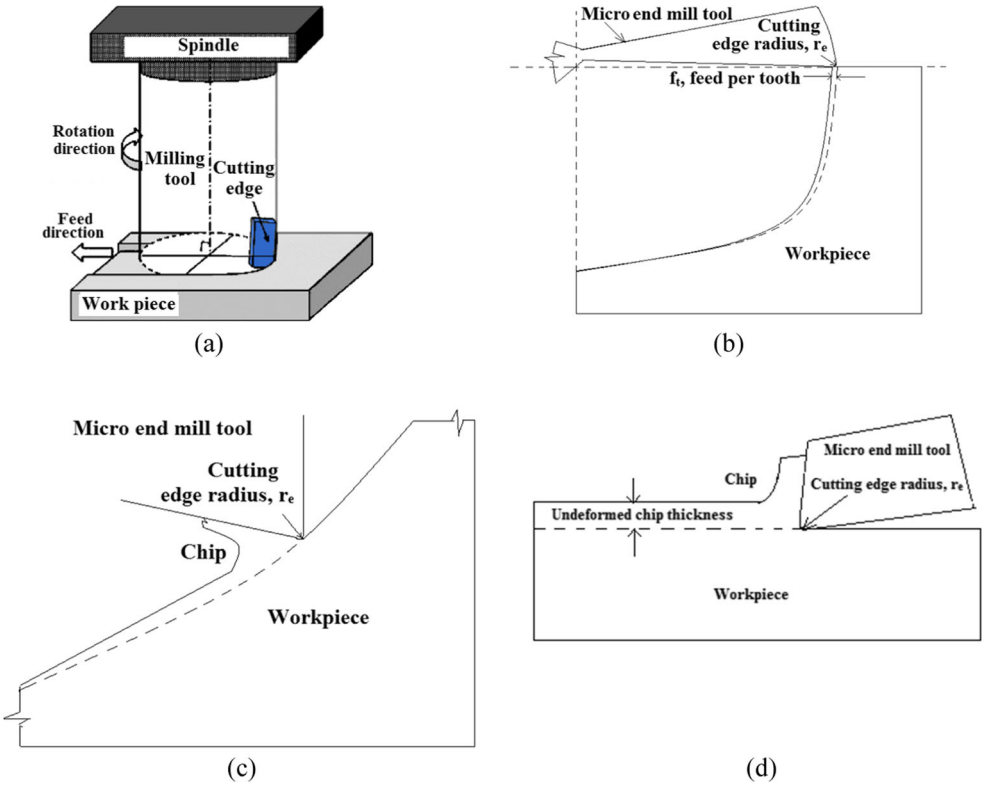

Fig. 6 Simplification for micro milling process (**a**) 3D milling process, (**b**) 2D representation of milling process, (**c**) Enlarged view of cutting zone, (**d**) Orthogonal machining representation [6]. © Elsevier. Reproduced by permission of Elsevier. Permission to reuse must be obtained from the rights holder

defining the effective rake angle. The effective rake angle becomes negative when the undeformed chip thickness is less than the minimum uncut chip thickness. Kang et al. [19] did not consider the cutting edge radius effect into their model. In this paper, the effect of the cutting edge radius of the tool has been accommodated into the model so that the proposed model can be used for predicting cutting forces at lower feed per tooth where the size effect due to the cutting edge radius plays a major role. For feed per tooth up to the size effect region, the effective rake angle was used and above that nominal tool rake angle was taken. Effective rake angle is defined as the angle between the vertical axis and tangent to the contact point between the cutting tool and the undeformed chip thickness [24] as shown in Fig. 7. The expression for calculating the effective rake angle is given in Eq. (14). Even though the effect of cutting edge radius on cutting force has been reported in literature [18, 25–27], the influence of the spring back effect on cutting force has not been considered. In this study, the Ti-6Al-4V titanium alloy was used as workpiece material, which got high spring back effect because of its high elasticity and small plastic deformation [28]. This bouncing action of Ti-6Al-4V during machining results in contact of workpiece on the flank face of the tool. In this study, the influence of spring back effect on cutting force has been considered.

$$\alpha = \sin^{-1}\frac{(r_e - t)}{r_e} \tag{14}$$

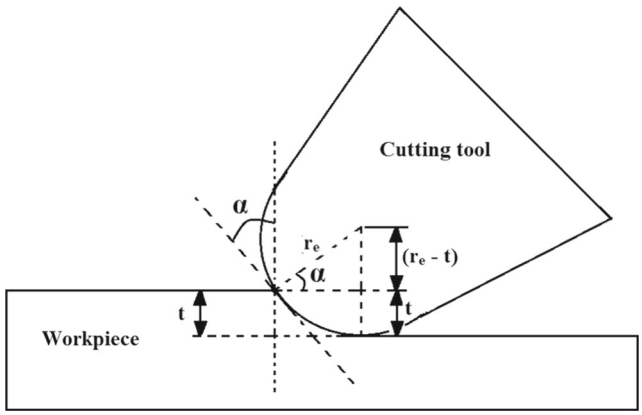

Fig. 7 Effective rake angle calculation (Ng et al. [24]). © Elsevier. Reproduced by permission of Elsevier. Permission to reuse must be obtained from the rights holder

α : Effective rake angle

r_e : Cutting edge radius

t : Undeformed chip thickness

4 Results and discussions

4.1 Cutting force

Figure 4 shows the experimental setup for acquiring force signal during the micro end milling process. The KISTLER 9256C2 dynamometer was attached to the machine in such a way that force components F_x, F_y, and F_z are measured as indicated in Fig. 8.

Since micro end mill tools with two flutes were used in this study, cutting force signals were analyzed for 180° rotation of the tool to understand the contribution of a single flute.

For the end milling process, the orthogonal thrust force (F_t) will be radial force (F_{rad}) and orthogonal cutting force (F_c) will have two components, longitudinal force F_{lon} and tangential force F_{tan}, as given in Eq. (15) and Eq. (16) [5].

$$F_{lon} = F_c \sin\psi \tag{15}$$

$$F_{tan} = F_c \cos\psi \tag{16}$$

In order to relate these forces to the force acquired from the dynamometer, F_t (or F_{rad}), F_{lon}, and F_{tan} need to be transformed to the Cartesian coordinate system. For any angular position θ of the cutting tool (Fig. 9), the end milling forces can be resolved into the Cartesian coordinate as given below:

$$F_x = F_r \sin\theta + F_c \cos\psi \cos\theta \tag{17}$$

$$F_y = F_r \cos\theta - F_c \cos\psi \sin\theta \tag{18}$$

Figure 10 shows variation of cutting force with feed per tooth for 0.10 mm depth of cut. It is clear from Fig. 10 that cutting force increases almost linearly with feed per tooth above 1 μm. However, for feed per tooth less than 1 μm cutting force deviates from the linear trend and gives a nonlinear behavior. The reason for this could be due to the fact that 1 μm falls in the range of minimum uncut chip thickness for the tool used in this study (cutting edge radius of the tool was approximately 3 μm). This result agrees with the findings of de Oliveira et al. [12], where the minimum uncut chip thickness was defined to be in the range of one fourth to one third of the cutting edge radius. When feed per tooth becomes less than the minimum uncut chip thickness, the cutting process is dominated by the ploughing process. This resulted in an increase in cutting force at lower undeformed chip thickness.

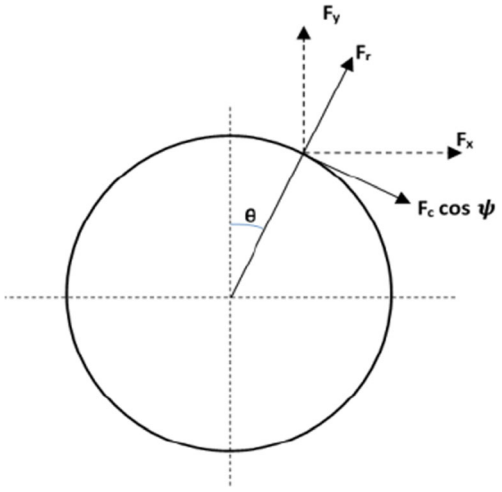

Fig. 9 Transformation of end milling forces to Cartesian coordinate system

4.2 Validation of cutting force model

In order to validate the force model developed in Section 3 to predict the micro end milling force, experiments were conducted for a wide range of feed/tooth on Ti-6Al-4V work piece material. Each experimental condition was repeated for three times and the average value is reported. Fresh tool data were used in all condition. Cutting forces F_x and F_y were calculated using Eq. (9) and Eq. (10). Flow stress of the work piece material was used based on the work by Lee et al. [14].

Figure 11 shows predicted and measured forces during micro end milling of Ti-6Al-4V. Forces were computed only for 180° rotation of the tool to study the contribution of single tooth. Predicted and measured forces F_x and F_y for 0.2, 0.4, and 0.6 μm feed/tooth are shown in Fig. 11. It can be noticed that force trend predicated by the model matches with the experimental results. Also, the predicted value is close to the

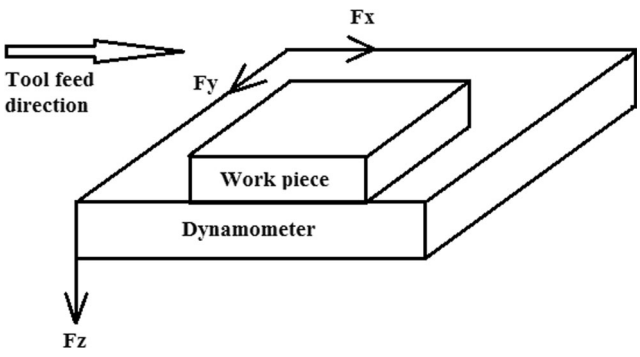

Fig. 8 Cutting force direction

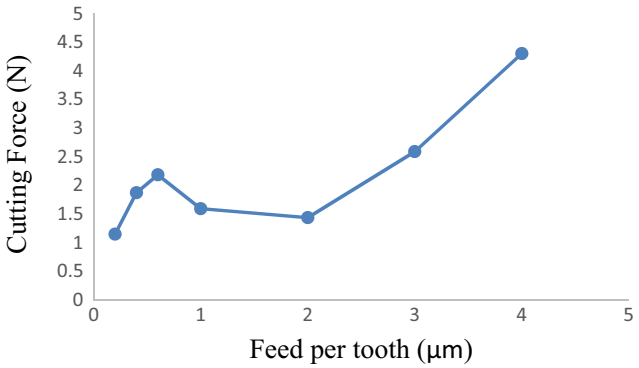

Fig. 10 Effect of undeformed chip thickness on cutting force

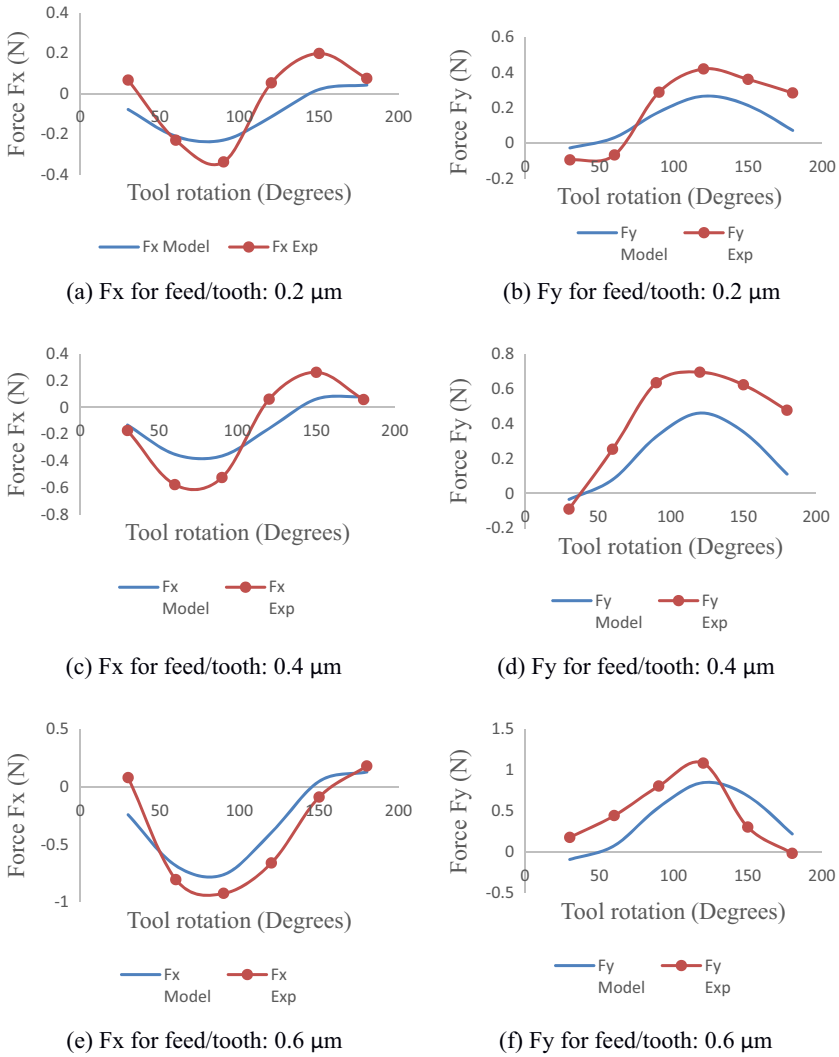

(a) Fx for feed/tooth: 0.2 µm

(b) Fy for feed/tooth: 0.2 µm

(c) Fx for feed/tooth: 0.4 µm

(d) Fy for feed/tooth: 0.4 µm

(e) Fx for feed/tooth: 0.6 µm

(f) Fy for feed/tooth: 0.6 µm

Fig. 11 Experimental and predicted micro end milling forces for feed rates of 0.2, 0.4, and 0.6 µm/tooth at cutting speed of 15.7 m/min and depth of cut of 0.1 mm. **a** F_x for feed/tooth, 0.2 µm. **b** F_y for feed/tooth, 0.2 µm. **c** F_x for feed/tooth, 0.4 µm. **d** F_y for feed/tooth, 0.4 µm. **e** F_x for feed/tooth, 0.6 µm. **f** F_y for feed/tooth, 0.6 µm

experimental results. Deviation from the experimental result may be due to tool wear, which was not taken into account in this study. Figure 12 shows a comparison between the new tool and condition of tool after cutting 20 mm length. It can be clearly observed that the cutting edge radius of the tool has increased due to tool wear when compared with the new tool. This would result in change in the minimum uncut chip thickness and thereby affects the effective rake angle. This could be the reason for deviation of experimental results from the model.

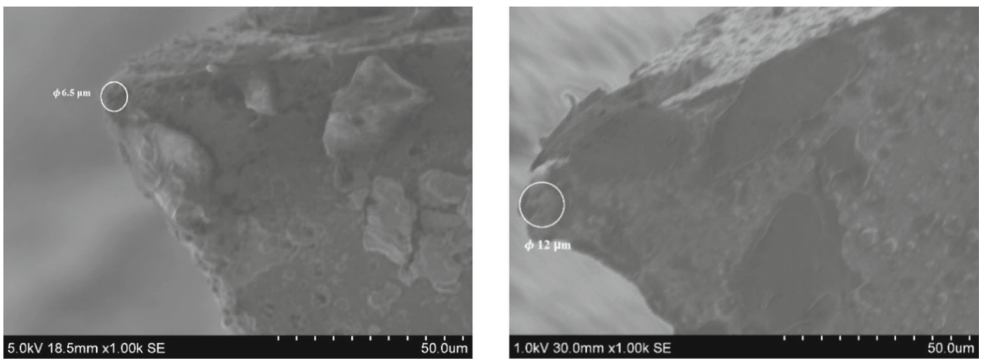

(a) New tool
(cutting edge diameter – 6.5 µm)

(b) Worn tool after 20 mm length of cut
(cutting edge diameter – 12 µm)

Fig. 12 Comparison between cutting edge radius of **a** new tool and **b** worn tool after 20 mm length of cut

However, at low feed per tooth values, it was observed that prediction error is more. This could be due to the following reasons as given below:

(a) At low feed per tooth, there is a possibility of frequent change over between ploughing- to shearing-dominant regimes during the micro end milling process [18] as shown in Fig. 13. This would result in vibration due to sudden change in the forces. This may be one of the reasons for the deviation between the experimental and predicted results at low feed per tooth values. It is reported in literature that during ploughing, the material flows three dimensionally which may result in tool deflection [18]. This effect will be predominant at low feed per tooth. This aspect is also not considered in this study and resulted in deviation between experimental and predicted values at low feed per tooth.

(b) Another important aspect of the micro end milling process which would result in increased cutting force at low feed per tooth is the dependence of strength on the scale of deformation [17, 29]. Various explanations have been reported that relate the size effect to the material strengthening mechanism such as (i) decreasing number of defects in micro structure [30], (ii) increase in the strain rate in the primary shear zone [31], (iii) increase in the shear strength of the workpiece material due to decrease in the tool-chip interface temperature [32]. In the micro end milling process when feed per tooth is within the size effect region, these effects will influence the cutting force and its effect will be predominant at low feed per tooth. This could be another reason for higher deviation between experimental and predicted results at lower feed per tooth.

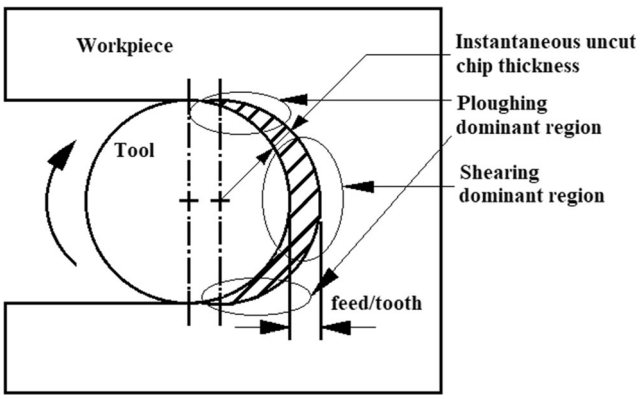

Fig. 13 Change over between the ploughing- to shearing-dominant regimes during the micro end milling process

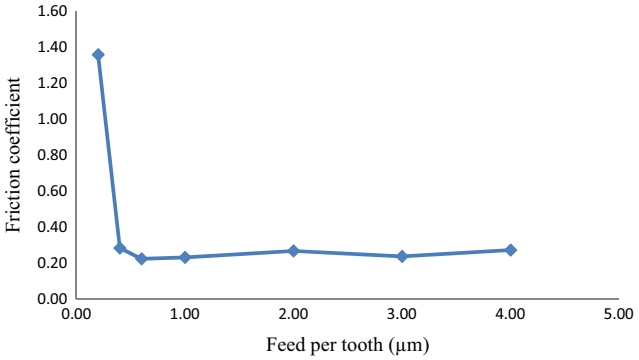

Fig. 14 Effect of feed per tooth on friction coefficient

4.3 Coefficient of friction

To investigate frictional size effect during the micro end milling process, a study on variation of coefficient of friction with feed per tooth has been carried out. Coefficient of friction between the tool rake face and chip can be calculated based on Eq. (12). In this study, the effective rake angle was used to calculate friction coefficient in order to incorporate size effect due to cutting edge radius.

From Fig. 14, it can be observed that friction coefficient increases with decrease in the feed per tooth. Similar trend was observed in Ng et al. [24] during the micro machining process.

Frictional size effect observed in this study can be visualized from Fig. 14. As feed per tooth decreases beyond the minimum uncut chip thickness, the friction coefficient was found to be increasing. In this study, the minimum chip thickness was found to be in the vicinity of 1 μm range from the cutting force analysis (Fig. 10). From Fig. 14, it can be noted that the coefficient of friction increases as feed per tooth falls below 1 μm. As feed per tooth reduces below the size effect zone, there is a variation in cutting force, as shown in Fig. 10; this gives rise to increase in coefficient of friction. Also, as feed per tooth decreases, the cutting temperature at tool-chip interface reduces, resulting in an increase of shear yield strength of workpiece material at tool-chip interface. This increase in shear yield strength

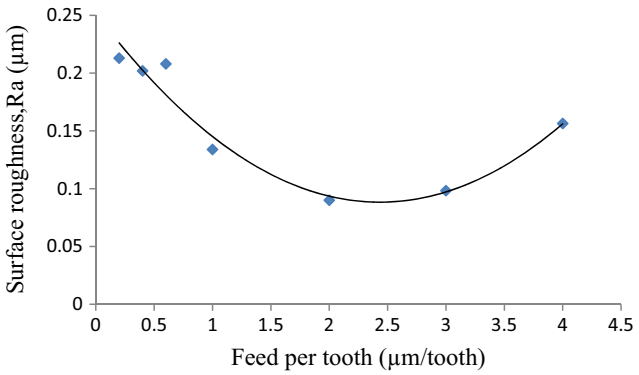

Fig. 15 Variation of surface roughness with feed per tooth

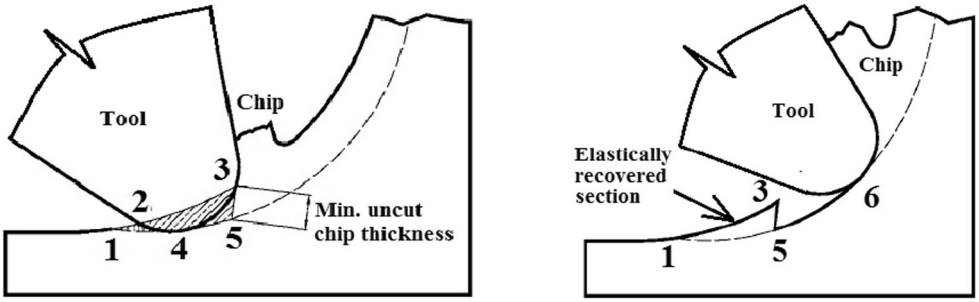

Fig. 16 Illustration of surface generation during micro machining considering minimum chip thickness effect. **a** Ploughing region. **b** Shearing region

of workpiece material at tool-chip interface contributes to increase of coefficient of friction [24].

4.4 Surface roughness

In order to study the effect of the cutting edge radius on the quality of the machined surface during the micro end milling process, an investigation on variation of surface roughness with feed per tooth was carried out. Surface roughness of the machined slot surface was characterized by using Surftest SJ – 410 (Mitutoyo) in terms of Ra value. Variation of surface roughness with feed/tooth is shown in Fig. 15. It can be observed that initially as feed per tooth increases, surface roughness decreases and reaches a minimum value and then

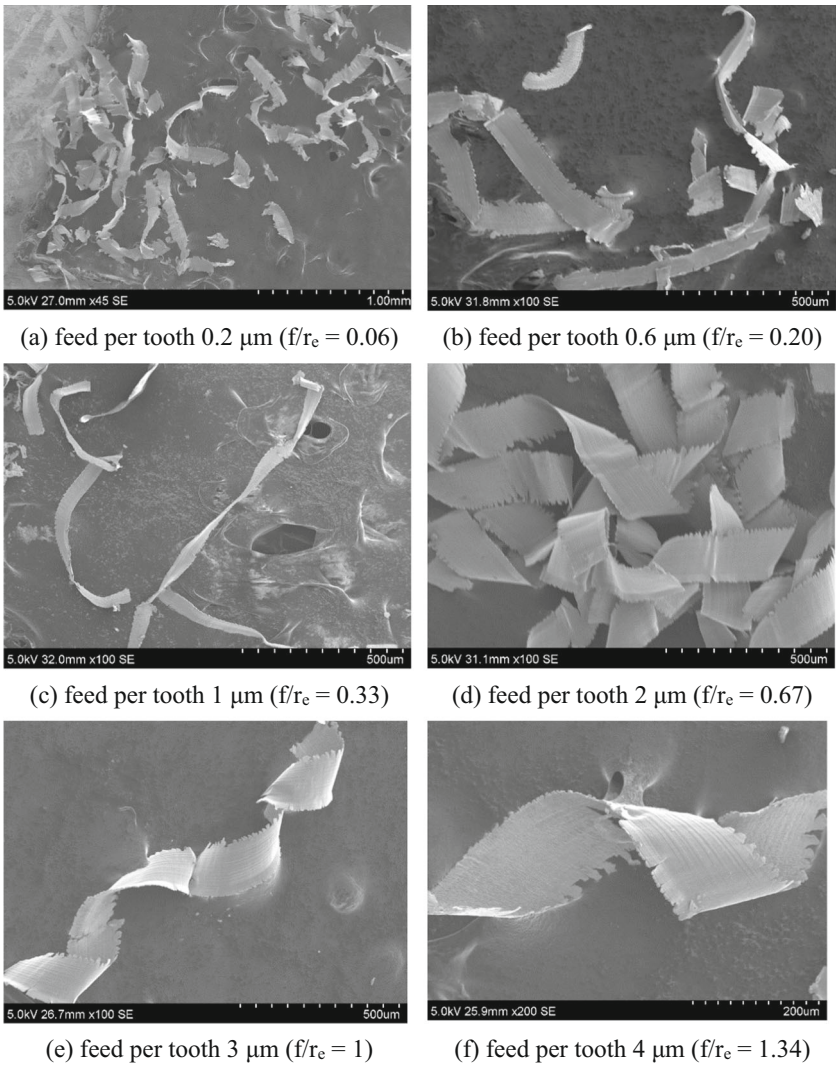

(a) feed per tooth 0.2 μm (f/r_e = 0.06)
(b) feed per tooth 0.6 μm (f/r_e = 0.20)
(c) feed per tooth 1 μm (f/r_e = 0.33)
(d) feed per tooth 2 μm (f/r_e = 0.67)
(e) feed per tooth 3 μm (f/r_e = 1)
(f) feed per tooth 4 μm (f/r_e = 1.34)

Fig. 17 Chip formation at selected feed per tooth during micro end milling process at cutting speed of 15.7 m/min and depth of cut 0.1 mm. **a** Feed per tooth 0.2 μm (f/r_e = 0.06). **b** Feed per tooth 0.6 μm (f/r_e = 0.20). **c** Feed per tooth 1 μm (f/r_e = 0.33). **d** Feed per tooth 2 μm (f/r_e = 0.67). **e** Feed per tooth 3 μm (f/r_e = 1). **f** Feed per tooth 4 μm (f/r_e = 1.34)

increases as feed per tooth increases. A similar trend was observed in Aramcharoen and Mativenga [4]. Figure 16 shows how minimum uncut chip thickness affects surface generation in the micro machining process. Surface 1-2-3 (Fig. 16a) represents machined surface after the previous tool path. Then, during the current tool pass, the cutting edge starts to engage the workpiece at 1 with uncut chip thickness equal to zero. As the tool moves along the path 1-4-5, uncut chip thickness gradually increases and reaches minimum uncut chip thickness at point 5 and the chip starts to generate. The workpiece material in the shaded area 1-2-3-5-4 (Fig. 16a) experiences ploughing and will not be removed since the uncut chip thickness is less than the minimum uncut chip thickness. As the tool moves as shown in Fig. 16b, the plowed material will be recovered to the original position 1-3 and generated surface after point 5 follows the tool path 5-6 because workpiece material is removed as chips. As a result, for feed per tooth is less than the minimum uncut chip thickness, surface roughness increases as feed per tooth reduces. For feed per tooth above the minimum chip thickness range, surface roughness increases as in the case of the macro end milling process.

4.5 Chip geometry

In micro machining, there exists a minimum uncut chip thickness (MUCT) which largely depends on the cutting edge radius of the tool, determining whether a chip is formed or not. For the undeformed chip thickness below MUCT, the cutting process is dominated by ploughing and above which shearing is dominated. In this study, an investigation on chips produced at various feed per tooth was carried out to understand the effect of the edge radius on machining mechanisms such as ploughing and shearing also on chip formation during the micro end milling process. In each test, machined chips were collected and imaged in SEM. In the micro end milling process, the size effect is mainly dependent on relationship between feed per tooth and tool edge radius. Therefore, by knowing the value of the cutting edge radius of the tool, it is possible to predict at which point chips will be generated during the machining process. Figure 17 shows a chip chart depicting various types of chips generated during the micro end milling process for a range of feed per tooth as 0.2, 0.6, 1, 2, 3, and 4 μm. Corresponding feed per tooth to cutting edge ratio is 0.06, 0.20, 0.33, 0.67, 1, and 1.34.

From Fig. 17a, b, it can be observed that particles collected from the workpiece during the micro end milling process cannot be classified as chip-like, as they possess various forms due to crushing and extruding processes caused by the predominant ploughing action present at lower feed per tooth.

From Fig. 17c–f, it can be observed that the material removed from the workpiece by the micro end milling process can be classified as chips. From this chip chart, it can be noted that feed per tooth of 1 μm can be considered to be an approximate range of minimum uncut chip thickness above which chips may be completely generated. For higher feed per tooth values (Fig. 17e–f), it can be observed that helical chips are generated. This is due to the fact that as feed per tooth value increases beyond the minimum uncut chip thickness value, the machining mechanism becomes similar to the macro end milling process.

5 Conclusion

In this study, an investigation on the effect of the cutting edge radius of the tool on cutting force, coefficient of friction, surface roughness, and chip formation during micro end milling of Ti-6Al-4V was carried out for a wide range of feed per tooth. Also, a force model considering the effect of cutting edge radius of the tool was presented and validated with the experimental results. Major conclusions made in this study are as follows:

- Cutting force was found to be increasing almost linearly with feed per tooth when machining at feed per tooth greater than the size effect zone.
- When feed per tooth is smaller than the size effect zone, cutting force is found deviate from the linear trend and gives an irregular force pattern.
- From cutting force versus feed per tooth graph (Fig. 10), the size effect zone was found to be in the range of 1 μm which is approximately one third of the cutting edge radius.
- Coefficient of friction, μ, was also found to be influenced by the size effect. For feed per tooth less than the size effect zone μ increases.
- While machining within the size effect region, surface roughness decreases with feed per tooth. Whereas above the size effect zone, surface roughness increases with feed per tooth as in the case of macro machining.
- The cutting force model proposed by Kang et al. [19] was modified by including the cutting edge radius effect, which is predominant in micro machining, during the micro end milling process, and has been experimentally validated.
- At very low feed per tooth, it was noticed that prediction error is more. This could be due to the fact that at low feed per tooth, the material strengthening effect and possibility of frequent change over between ploughing- to shearing-dominant regimes, have significant influence on cutting force which were not considered in this study.
- Chip chart has been prepared. It was observed that chips started forming at feed per tooth of 1 μm indicating transition from ploughing to shearing mechanism.

- Effect of tool wear during the micro end milling studies has been considered for future scope of work.

Acknowledgements Authors would like to sincerely thank the Department of Science and Technology (DST), Govt. of India and Centre for Precision Measurements and Nanomechanical Testing, Department of Mechanical Engineering, National Institute of Technology Calicut, for providing support to carry out this work under the scheme "Fund for Improvement of Science and Technology" (No. SR/FST/ETI-388/2015). Also, authors sincerely thank Dr. Basil Kuriachen, Assistant Professor, Mechanical Engineering Department, NIT MIZORAM, for his contribution during initial stages of this study.

References

1. Jin X, Altintas Y (2012) Prediction of micro-milling forces with finite element method. J Mater Process Technol 212:542–552
2. Zaman MT, Kumar AS, Rahman M, Sreeram S (2006) A three-dimensional analytical cutting force model for micro end milling operation. Int J Mach Tools Manuf 46:353–366
3. Malekian M, Park SS, Jun MBG (2009) Modeling of dynamic micro-milling cutting forces. Int J Mach Tools Manuf 49:586–598
4. Aramcharoen A, Mativenga PT (2009) Size effect and tool geometry in micromilling of tool steel. Precis Eng 33:402–407
5. Bissacco G, Hansen HN, Slunsky J (2008) Modelling the cutting edge radius size effect for force prediction in micro milling. CIRP Ann Manuf Technol 57:113–116
6. Lai X, Li H, Li C, Lin Z, Ni J (2008) Modelling and analysis of micro scale milling considering size effect, micro cutter edge radius and minimum chip thickness. Int J Mach Tools Manuf 48:1–14
7. Vogler MP, Kapoor SG, DeVor RE (2004) On the modeling and analysis of machining performance in micro-end milling, part II: cutting force prediction. J Manuf Sci Eng 126:695–705
8. Vogler MP, DeVor RE, Kapoor SG (2004) On the modeling and analysis of machining performance in micro-end milling, part I: surface generation. J Manuf Sci Eng 126:685–694
9. Liu X, DeVor RE, Kapoor SG (2006) An analytical model for the prediction of minimum chip thickness in micromachining. Trans ASME 128:474–481
10. Malekian M, Mostofa MG, Park SS, Jun MBG (2012) Modeling of minimum uncut chip thickness in micro machining of aluminum. J Mater Process Technol 212:553–559
11. Zhanqiang L, Zhenyu S, Yi W (2013) Definition and determination of the minimum uncut chip thickness of micro cutting. Int J Adv Manuf Technol 69:1219–1232
12. de Oliveira FB, Rodrigues AR, Coelho RT, deSouza AF (2015) Size effect and minimum chip thickness in micromilling. Int J Mach Tools Manuf 89:39–54
13. Sooraj VS, Mathew J (2011) An experimental investigation on the machining characteristics of microscale end milling. Int J Adv Manuf Technol 56:951–958
14. Lee WS, Lin CF (1998) Plastic deformation and fracture behavior of Ti–6Al–4V alloy loaded with high strain rate under various temperatures. Mater Sci Eng A 241:48–59
15. Mamedov A, Lazoglu I (2016) Thermal analysis of micro milling titanium alloy Ti–6Al–4V. J Mater Process Technol 229:659–667
16. Arcona C, Dow TA (1998) An empirical tool force model for precision machining. Trans ASME 120:700–707
17. Afazov SM, Zdebski D, Ratchev SM, Segal J, Liu S (2013) Effects of micro-milling conditions on the cutting forces and process stability. J Mater Process Technol 213:671–684
18. Jun MBG, Goo C, Malekian M, Park SS (2012) A new mechanistic approach for micro end milling force modeling. J Manuf Sci Eng 134:011006-1–011006-9
19. Kang IS, Kim JS, Kim JH, Kang MC, Seo YW (2007) A mechanistic model of cutting force in the micro end milling process. J Mater Process Technol 187–188:250–255
20. Kumar M, Chang CJ, Melkote SN, Joseph R (2013) Modeling and analysis of forces in laser assisted micro milling. J Manuf Sci Eng 135:041018–1–041018–10
21. Park SS, Malekian M (2009) Mechanistic modeling and accurate measurement of micro end milling forces. CIRP Ann Manuf Technol 58:49–52
22. Srinivasa YV, Shunmugam MS (2013) Mechanistic model for prediction of cutting forces in micro end-milling and experimental comparison. Int J Mach Tools Manuf 67:18–27
23. Afazov SM, Ratchev SM, Segal J (2010) Modelling and simulation of micro-milling cutting forces. J Mater Process Technol 210:2154–2162
24. Ng CK, Melkote SN, Rahman M, Kumar AS (2006) Experimental study of micro- and nano-scale cutting of aluminum 7075-T6. Int J Mach Tools Manuf 46:929–936
25. Rao S, Shunmugam MS (2012) Analytical modeling of micro end milling forces with edge radius and material strengthening effects. Mach Sci Technol: Int J 16:205–227
26. Anand RS, Patra K, Steiner M, Biermann D (2017) Mechanistic modeling of micro-drilling cutting forces. Int J Adv Manuf Technol 88:241–254
27. Anand RS, Patra K (2017) Mechanistic cutting force modelling for micro-drilling of CFRP composite laminates. CIRP J Manuf Sci Technol 16:55–63
28. Pramanik A (2012) Problems and solutions in machining of titanium alloys. Int J Adv Manuf Technol 70:919–928
29. Liu K, Melkote SN (2006) Material strengthening mechanisms and their contribution to size effect in micro-cutting. J Manuf Sci Eng 128:730–738
30. Backer WR, Marshall ER, Shaw MC (1952) The size effect in metal cutting. Trans ASME 74:61–72
31. Larsen-Basse J, Oxley PLB (1973) Effect of strain-rate sensitivity on scale phenomenon in chip formation. In: Proceedings of the 13th international machine tool design & research conference, University of Birmingham 209–216
32. Kopalinsky EM, Oxley PLB (1984) Size effects in metal removal process. In: Institute of physics conference series No. 70, third conference on mechanical properties at high rates of strain 389–396